Obtaining breathers in nonlinear Hamiltonian lattices

S. Flach*
Max-Planck-Institut für Physik Komplexer Systeme, Bayreuther Strasse 40, H 16, D-01187 Dresden, Germany
(Received 2 November 1994)

We present a numerical method for obtaining high-accuracy numerical solutions of spatially localized time-periodic excitations on a nonlinear Hamiltonian lattice. We compare these results with analytical considerations of the spatial decay. We show that nonlinear contributions have to be considered, and we obtain very good agreement between the latter and numerical results. We discuss further applications of the method and results.

PACS number(s): 03.20.+i, 63.20.Pw, 63.20.Ry

I. INTRODUCTION

The interest in the existence and properties of nonlinear localized excitations (NLE's) in Hamiltonian lattices has considerably increased since the work of Takeno *et al.* ([1, 2], and references therein). The NLE's are classical solutions and represent localized vibrations of the constituents (particles) of the Hamiltonian lattice. NLE's are thus similar to breather solutions of the sine-Gordon equation (a partial differential equation) and sometimes called discrete breathers. Remarkably, the lattice exhibits discrete translational invariance, i.e., no defects or disorder are present. Then the only reason for the possibility of the existence of NLE's is the nonlinearity of the system together with its discreteness. The nonlinearity is needed in order to be able to tune oscillatory frequencies by changing the energy or amplitude. The discreteness guarantees a finite bandwidth of the frequency band of small-amplitude linearized extended excitations (phonons). Consequently one can avoid resonances between the phonon band and the frequencies of NLE solutions.

Recently, the problem of finding time-periodic NLE solutions on Hamiltonian lattices was reformulated into finding appropriate solutions of a set of coupled algebraic equations [3]. The variables of this set are the Fourier coefficients of the NLE solution. This approach opens several possibilities to obtain analytical and numerical results for NLE's. In particular, spatial decay laws for every Fourier coefficient are derived, based on a linearization procedure [3].

In the present work we will first formulate a new mapping in order to numerically solve the mentioned set of algebraic equations. We obtain high-precision numerical solutions for these equations. The level of accuracy allows us to check analytical predictions. Next we reconsider the spatial decay problem of the NLE solution and find that under certain conditions the previously applied linearization procedure does not hold without exceptions. We obtain nonlinear corrections and formulate conditions for their restricted applicability. Finally we make use of the availability of high-precision numerical solutions and test our analytical predictions.

II. FORMULATION OF THE PROBLEM

We consider a system of classical interacting particles arranged on a certain lattice. By that we mean that the positions of all particles in the ground state (potential minimum) define a regular lattice structure. The potential energy of the system, expressed in the relative displacements of the particles from their ground state positions, exhibits a minimum if all displacements are zero. Since we are interested in the easiest demonstration of what we might call a general phenomenon, we restrict ourselves to the case of a one-dimensional lattice with one degree of freedom per unit cell. Also we choose nearest neighbor interaction. We show later that these restrictions are at best of some technical use, i.e., more complicated systems will exhibit the same behavior. The Hamilton function of our system can then be given in the form

$$H = \sum_l \left[\frac{1}{2} P_l^2 + V(X_l) + \Phi(X_l - X_{l-1}) \right] . \tag{1}$$

Here P and X denote the canonically conjugated momentum and displacement of a particle and the label l counts the unit cells. The on-site potential $V(z)$ and the interaction potential $\Phi(z)$ can be chosen in a Taylor expansion representation:

$$V(z) = \sum_{\alpha=2,3,\ldots} \frac{v_\alpha}{\alpha!} z^\alpha \ , \tag{2}$$

$$\Phi(z) = \sum_{\alpha=2,3,\ldots} \frac{\phi_\alpha}{\alpha!} z^\alpha \ . \tag{3}$$

Finally the equations of motion are given by

$$\ddot{X}_l = -\frac{\partial H}{\partial X_l} \ . \tag{4}$$

We search for a solution of (4) in the form

$$X_l(t) = X_l(t + T_1) \ , \ X_{l \to \pm\infty} \to 0 \ . \tag{5}$$

*Electronic address: flach@idefix.mpipks-dresden.mpg.de

If solution (5) exists, we can introduce a Fourier series representation for $X_l(t)$:

$$X_l(t) = \sum_{k=-\infty}^{+\infty} A_{kl} e^{ik\omega_1 t} \quad , \tag{6}$$

where $\omega_1 = 2\pi/T_1$. Let us separate the linear terms in the displacements X on the right hand side of (4) from the nonlinear ones:

$$\ddot{X}_l = -v_2 X_l - \phi_2(2X_l - X_{l-1} - X_{l+1}) + F_l^{(\mathrm{nl})}(X_{l'}) \quad . \tag{7}$$

The nonlinear part $F_l^{(\mathrm{nl})}$ of the force contains only higher than linear terms in the displacements:

$$F_l^{(\mathrm{nl})} = -\sum_{\alpha=3,4,\ldots} \left[\frac{v_\alpha}{(\alpha-1)!} X_l^{\alpha-1} + \frac{\phi_\alpha}{(\alpha-1)!}[(X_l - X_{l-1})^{\alpha-1} - (X_{l+1} - X_l)^{\alpha-1}] \right] \quad . \tag{8}$$

Since all functions $X_l(t)$ of our proposed solution (5) are periodic with the same period T_1, we can also expand $F_l^{(\mathrm{nl})}$ into a Fourier series:

$$F_l^{(\mathrm{nl})}(t) = \sum_{k=-\infty}^{+\infty} F_{kl}^{(\mathrm{nl})} e^{ik\omega_1 t} \quad . \tag{9}$$

The Fourier coefficients $F_{kl}^{(\mathrm{nl})}$ will be some functions of the coefficients $A_{k'l'}$ from (6) [depending on the given form of the potential functions (2) and (3)]. Inserting (6) into (4) and using (9) we finally obtain

$$k^2\omega_1^2 A_{kl} = v_2 A_{kl} + \phi_2(2A_{kl} - A_{k,l-1} - A_{k,l+1}) + F_{kl}^{(\mathrm{nl})} \quad . \tag{10}$$

The infinite set of equations (10) (for all k) represents a coupled set of equations for the Fourier coefficients A_{kl}.

This set of equations has to be analyzed in order to obtain nonlinear localized excitations, i.e. [cf. (5)], solutions with

$$A_{k,l\to\pm\infty} \to 0 \quad . \tag{11}$$

Let us briefly review what is known about the solutions of (10) with condition (11). In [4] it was shown that the finding of a nonlinear localized excitation is equivalent to obtaining common points (homoclinic points) of two separatrix manifolds of a certain mapping. It was also shown there that, if a solution can be found for a given system, then it is structurally stable with respect to perturbations of the Hamilton function and thus of generic type. Also in [4] an existence proof of NLE's was given for a system with $V(z) = 0$ and $\Phi(z) = (1/2m)z^{2m}$ $(m = 2, 3, \ldots)$. Furthermore, MacKay and Aubry [5] have shown that in the limit of weak interaction $\Phi(z)$ and any anharmonic potential $V(z)$ NLE's exist, remarkably for any lattice dimension, and also for larger interaction ranges and numbers of degrees of freedom per unit cell. Consequently the above considered simplest case is not different from more complicated (and therefore more realistic) models. A systematic study of one-dimensional [6, 7] and two-dimensional [8] lattices shows that there is no qualitative difference in the appearance and properties of NLE's.

III. THE METHOD OF FINDING SOLUTIONS — DESIGNING A MAP

Let us reformulate Eq. (10) into a map in order to obtain a numerical procedure for finding NLE solutions. For that we rewrite (10) in two ways:

$$A_{kl}^{(i+1)} = \frac{1}{k^2\omega_1^2}[(v_2 + 2\phi_2)A_{kl}^{(i)} - \phi_2(A_{k,l-1}^{(i)} + A_{k,l+1}^{(i)}) + F_{kl}^{(\mathrm{nl})}(A_{k'l'}^{(i)})] \quad , \tag{12}$$

$$A_{kl}^{(i+1)} = \frac{1}{v_2}[(k^2\omega_1^2 - 2\phi_2)A_{kl}^{(i)} + \phi_2(A_{k,l-1}^{(i)} + A_{k,l+1}^{(i)}) - F_{kl}^{(\mathrm{nl})}(A_{k'l'}^{(i)})] \quad . \tag{13}$$

Here the notation of the upper labels $(i+1)$ and (i) can be ignored for a moment. For clarity we explicitly indicate in (12) and (13) the dependence of the coefficients $F_{kl}^{(\mathrm{nl})}$ on the coefficients A_{kl}. Both Eqs. (12) and (13) are equivalent to each other with respect to solutions. If we now take into account the upper labels $(i+1)$ and (i), then these two equations in fact become two maps. Given the coefficients A_{kl} at the ith step, we can calculate the coefficients A_{kl} at the $(i+1)$st step. If we find a fixed point of any of the two maps, then it will also be a fixed point of the second map. Each fixed point of these maps is a solution of the original Eq. (10).

One fixed point can be immediately found — it is $A_{kl} = 0$ for all k, l. If we linearize the map around this fixed point and assume for a moment $\phi_2 = 0$ we obtain the eigenvalues

$$\lambda_{kl}^{(12)} = \frac{v_2}{k^2\omega_1^2} \quad , \tag{14}$$

$$\lambda_{kl}^{(13)} = \frac{k^2\omega_1^2}{v_2} = \frac{1}{\lambda^{(12)}} \quad . \tag{15}$$

Here the upper labels of the eigenvalues indicate the equation number of the map they belong to. If now ϕ_2 is smoothly increased from zero, then the eigenvalues (14) and (15) will also smoothly change [9]. Consequently, we might expect some control over the values of the eigenvalues in the case of nonzero interaction. As for the eigenvectors, any orthonormal set of basis vectors would be an eigenvector base for the linearized maps in the case $\phi_2 = 0$. For clarity we can always choose the eigenvector set which appears in the limit $\phi_2 \to 0$. Then the eigenvectors are also smoothly changed by increasing ϕ_2 from zero.

As follows from (15), both eigenvalues for a given pair of (k, l) are positive and inverse to each other. Consequently one of the eigenvalues will be larger than 1 and the second eigenvalue will be smaller than 1. In order to find a NLE solution we design a new map out of the two maps (12) and (13). This new map can be composed

out of the two maps (12) and (13) in an appropriate way depending on the given problem one wants to solve. Let us explain the strategy of this designing. Suppose we want to find a NLE solution with a given frequency ω_1, which is centered on a lattice site $l = 0$. Then we choose out of the two maps (12) and (13) the one which yields an eigenvalue larger than 1 for the pair $(k = \pm 1, l = 0)$ according to (12) and (13). For all other pairs (k, l) we choose the map which yields an eigenvalue smaller than 1 (note that this choice might still be different for different k). By that we achieve the following. If we choose as an initial condition for our designed map a set of the A_{kl} with $A_{k=\pm 1,l=0} = \delta$, $A_{k\neq\pm 1,l\neq 0} = 0$, then we can expect that starting iterating our map we essentially get growth in the direction of the unstable eigenmode at $(k = \pm 1, l = 0)$, whereas all other eigenmodes are not excited (eigenvalues lower than 1). Because we have designed a map in which the translational invariance with respect to l is broken at $l = 0$, we also know that the corresponding eigenvector is of local character for small ϕ_2. A way to estimate whether this statement is correct is to calculate the ratio of the off-diagonal terms in the linearized map (which is roughly given by ϕ_2/v_2) over the difference between the diagonal terms:

$$\frac{\phi_2}{v_2}\left(\frac{v_2}{\omega_1^2} - \frac{\omega_1^2}{v_2}\right) = \frac{\phi_2\omega_1^2}{v_2^2 - \omega_1^4} \quad . \tag{16}$$

This ratio has to be small enough to be sure that the above given arguments hold. Once our iteration yields local growth for the Fourier coefficients, we can hope that the nonlinear terms of the map, which become important for large enough A_{kl}, will lead the iteration to the fixed point which corresponds to a NLE solution. There is absolutely no guarantee that that will happen. We have no knowledge about the properties of this fixed point, even if we know for sure that the NLE solution exists (which means, in turn, that the fixed point exists). All the designing is focusing on is to get the right initial growth (namely, local growth) in our iteration.

If we were to search for a NLE which is centered between two lattice sites $l = 0, 1$, all we would have to change is to add an unstable map for the pair $k = \pm 1, l = 1$, and, depending on the symmetry of the solution (in-phase or out-of-phase motion), to choose equal or opposite signs for the initial perturbations in $A_{k=\pm 1,l=0}$ and $A_{k=\pm 1,l=1}$.

IV. SOLUTIONS

We implemented two numerical realizations for the designed map. The main difficulty is to account for the nonlinear terms $F_{kl}^{(\mathrm{nl})}$ (9). In this paper we report on results for systems with $V(z)$ and $\Phi(z)$ being finite order polynomials in z. Then one way of calculating the nonlinear terms is to evaluate all possible combinations of products of the Fourier coefficients A_{kl}. We will call this method the *polynomial approach*. As an example we give the contribution of the first term in the sum on the right hand side of Eq. (8):

$$F_{kl}^{(\mathrm{nl})} = \sum_{\alpha=3,4,\ldots} \frac{v_\alpha}{(\alpha-1)!} \times \sum_{k_1,k_2,\ldots,k_{\alpha-1}=-\infty}^{+\infty} A_{k_1 l}A_{k_2 l}\cdots A_{k_{\alpha-1} l} \times \delta_{k,(k_1+k_2+\cdots+k_{\alpha-1})} \quad . \tag{17}$$

Here $\delta_{a,b}$ stand for the Kronecker symbol with integer a, b.

The polynomial approach can become very inefficient if the number and order of nonlinear terms in (17) become large (in fact $\alpha = 5$ can already pose serious computing problems). If the potential functions are not given by finite order polynomials then the polynomial approach breaks down. In this case it is more useful to numerically integrate the function $F_l^{(\mathrm{nl})}(t)$:

$$F_{kl}^{(\mathrm{nl})} = \frac{1}{T_1}\int_{-T/2}^{T_2} F_l^{(\mathrm{nl})}(t)e^{-ik\omega_1 t}dt \quad . \tag{18}$$

We will call this approach the *Fourier integral approach*. Here $T_1 = 2\pi/\omega_1$ is the period of the NLE solution. If we know A_{kl} for all (k, l), then we can immediately calculate (18) using (8). In order to test the accuracy of our calculations we can use both approaches and thus compare the two results, which have to be equivalent.

Another important restriction on the numerical approach is the finiteness of the k sums. We have to introduce by hand a cutoff in k space: $A_{kl} = 0$ for $|k| \geq k_{\max}$. This cutoff will be justified only if the numerically evaluated Fourier coefficients A_{kl} drop to small enough values at the cutoff $k_{\max}$. Here "small enough" will be defined through the accuracy of the numerical calculations. We will stop the iteration if the sum

$$\sum_{k,l} |A_{kl}^{(i)} - A_{kl}^{(i-1)}| < 10^{-10} \quad . \tag{19}$$

In this paper we will study three models. Model I is characterized by $V(z) = 1/2z^2 - 1/4z^4$ and $\Phi(z) = 1/2Cz^2$. Model II has the potential functions $V(z) = z^2 - z^3 + 1/4z^4$, $\Phi(z) = 1/2Cz^2$. Model III is defined through $V(z) = 1/2z^2 + 1/4z^4$, $\Phi(z) = 1/2Cz^2$. Model I is characterized by a local minimum for $z = 0$ and a global instability for $|z| \geq 1$. Here we will restrict ourselves to small enough amplitudes such that we avoid the instability region. Model II is the well known Φ^4 lattice model [after a change of variables $z' = z - 1$ one arrives at the symmetric form of the double-well on-site potential $V(z') = 1/4(z'^2 - 1)^2$]. This model has in fact two identical ground states, $z' = \pm 1$ or $z = 0, 2$. Without loss of generality we have chosen $z' = -1$ as the ground state around which we expand the potential functions. Model III differs from Model I by the sign in front of the quartic term in $V(z)$. Consequently there is no instability in this model. In all models the parameter $C = \phi_2$ regulates the bandwidth of phonons obtained after a linearization of the equations of motion around the ground state:

$$v_2 \leq \omega_q^2 \leq v_2 + 4C \quad . \tag{20}$$

Here ω_q is the frequency of a phonon wave with wave

number q. For our models we have the following: model I, $v_2 = 1$; model II, $v_2 = 2$; model III, $v_2 = 1$. In our calculations we will use $C = 0.1$.

In all three model cases the phonon band has a nonzero lower band edge v_2. In order to solve the map for the Fourier coefficients we have to know (or be able to predict) whether the NLE frequency can be below or above the phonon band (or maybe below and above). There exists a rather straightforward method to do so. First we have to know the symmetry of the solutions with respect to their position on the lattice. In most cases (even supported by rigorous proofs for some cases) we can expect two solutions: a NLE centered on a lattice site (meaning that the center of energy of the energy distribution of the solution has a maximum on a lattice site) which we call the XC solution; and a NLE centered between two lattice sites which we call the XN solution (this notation was first used in [10]). Now all one has to do is to consider two possibilities: that the NLE frequency might be below or above the phonon band. As was shown in [3], this option defines whether the motion of particles in the solution is of in- or out-of-phase character. In [6, 8] it was explained how to construct a certain effective potential out of this input information. The motion of a particle in this effective potential can then be analyzed with respect to the energy dependence of its oscillation frequency. This energy dependence is qualitatively (and often even quantitatively) the same as the energy dependence of the NLE. If, e.g., the initial assumption was "frequency below the phonon band," but the effective potential yields only frequencies above the phonon band, then the initial assumption was wrong (and vice versa). Let us give the form of the effective potentials for the four different cases:

$$V_{\rm eff}(z) = V(z) + \Phi(z) + \Phi(-z) \ , \ \text{XC} \ , \quad \omega_1 < \omega_q \ , \tag{21}$$

$$V_{\rm eff}(z) = 2V(z) + \Phi(z) + \Phi(-z) \ , \ \text{XN} \ , \quad \omega_1 < \omega_q \ , \tag{22}$$

$$V_{\rm eff}(z) = V(z) + \Phi(z) + \Phi(-z) \ , \ \text{XC} \ , \quad \omega_1 > \omega_q \ , \tag{23}$$

$$V_{\rm eff}(z) = V(z) + V(-z) + \Phi(2z) + \Phi(z) + \Phi(-z) \ , \ \text{XN}, \quad \omega_1 > \omega_q \ . \tag{24}$$

As follows from the analysis, model I allows only for cases (21) and (22) ($\omega_1 < \omega_q$). For model III we find the reverse case $\omega_1 > \omega_q$. For model II and small energies we find $\omega_1 < \omega_q$, whereas for large energies also $\omega_1 > \omega_q$ can be realized.

Having this information, we can proceed with the numerical treatment of the map for the Fourier coefficients. In Fig. 1 we show an XC NLE solution as obtained for model I and the frequency $\omega_1 = 0.8$. We used periodic boundary conditions (PBC), 100 lattice sites, and $k_{\rm max} = 30$. Because of the symmetry of the potential functions all Fourier coefficients with even k vanish. In our calculations (both with the polynomial and the Fourier integral approach), however, we did not use this information. Both methods yield exactly the same solution; in particular, the even Fourier coefficients indeed vanish. In Fig. 1 the dependence of $|A_{kl}|$ on the lattice site l is shown in a semilogarithmic plot. The actual data are given as open squares. Data for equal values of k are connected with solid lines. The value of k increases from top to bottom: $k = 1, 3, 5, \ldots$. As is clearly seen in Fig. 1, Fourier coefficients for each k show up with a logarithmic decay in l. What is not observable in the plot of Fig. 1 is that the Fourier coefficents for a given k alternate their signs as one increases or decreases l by 1. Only for $k = 1$ is the sign of all A_{1l} the same, independent of l. The Fourier coefficients for negative k are identical to the corresponding coefficents for positive k: $A_{kl} = A_{-k,l}$. Let us also mention that we have checked any finite size effects. We have computed the same solution for 30 lattice sites, and found *practically no* difference in the values of the Fourier coefficients. This appears to be logical, since the solution we find is very localized, so that it does not matter how large the system is. Consequently, we can be sure that we find a solution which is also a solution of the infinite problem.

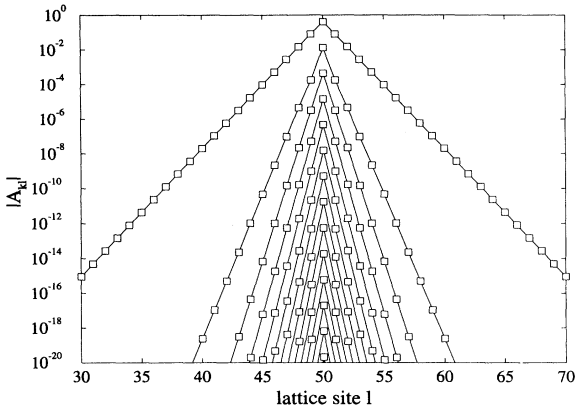

FIG. 1. Numerical result for an XC NLE solution for model I (see text). Open squares are numerical data. Lines connect Fourier coefficients with same value of k.

In Fig. 2 we show an XN NLE solution for the same model I, where all other parameters are as in the case of

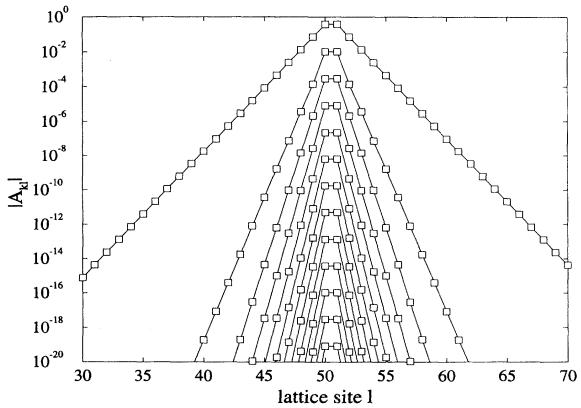

FIG. 2. Same as in Fig. 1 but for an XN NLE solution.

the solution in Fig. 1. All the comments from Fig. 1 apply to Fig. 2.

Let us consider model II. We choose a frequency $\omega_1 = 1.3$ which is below the phonon band. Because of the asymmetry of the corresponding on-site potential $V(z)$ Fourier components with even k will be nonzero. The result for an XC NLE is shown in Fig. 3. Data belonging to one k value are again connected with solid lines. The value for k from top to bottom is $k = 1, 0, 2, 3, 4, \ldots$. The signs of A_{kl} are positive for $k = 0, 1, 3$, negative for $k = 2$, and alternating for all other k values. We also created a similar XN NLE solution with the same frequency for model II which behaves similarly to the XC solution in Fig. 3.

In Fig. 4 we show the result for an XC NLE solution for model III. Here the frequency $\omega_1 = 1.3$ is chosen to be above the phonon band. As in the case of model I the symmetry of the potential functions causes all even k Fourier coefficients to vanish. The k values for the nonzero odd k Fourier coefficients in Fig. 4 increase from top to bottom: $k = 1, 3, 5, \ldots$. For all odd k values the signs of the Fourier coefficients alternate as we change the lattice site l by 1. Again we also created a similar XN NLE solution.

V. THE SPATIAL DECAY RECONSIDERED

In [3] the spatial decay of the Fourier components A_{kl} was studied. The main idea was to start with (10) and rewrite it in the form

$$A_{k,l+1} = \frac{v_2}{\phi_2} A_{kl} + 2A_{kl} - A_{k,l-1} - \frac{k^2\omega_1^2}{\phi_2} A_{kl} + \frac{1}{\phi_2} F_{kl}^{(\mathrm{nl})} \quad . \tag{25}$$

Equation (25) can be interpreted as a map: knowing all Fourier coefficients at lattice sites l and $(l-1)$ one can calculate the coefficients at $(l+1)$. Naturally one can iterate also to negative values of l [i.e., one just exchanges $(l+1)$ with $(l-1)$ in (25)]. If we iterate into the tails of a NLE solution, then because of (11) it was suggested in [3] that the nonlinear contributions $F_{kl}^{(\mathrm{nl})}$ which are at least of second order in $A_{k'l'}$ can be neglected. Then Eq. (25) is transformed into an infinite set of two-dimensional maps for each value of k. As a result exponential decay laws are obtained [3]:

$$A_{kl} \sim [\mathrm{sgn}(\lambda_k)]^l \, e^{\ln|\lambda_k| l} \quad , \tag{26}$$

$$\lambda_k = 1 + \frac{\kappa_k(\omega_1)}{2} \pm \sqrt{\left(1 + \frac{\kappa_k(\omega_1)}{2}\right)^2 - 1} \quad , \tag{27}$$

with $\kappa_k(\omega_1) = (v_2 - k_1^2\omega_1^2)/(\phi_2)$. The sign in (27) hase to be chosen in order to obey the condition $|\lambda_k| \leq 1$. One of the interesting properties of (27) is that all one has to know about the problem is the frequency of the NLE solution and the positions of the phonon band which are given by (v_2, ϕ_2). Consequently, several predictions were drawn in [3] on this basis which were successfully checked.

However, in order to justify the dropping of the nonlinear contributions in (25) one has to insert the predicted decay laws as obtained from the linearization into the full equations and show that the nonlinear terms are indeed negligible. Let us consider the contributions of the nonlinear terms as given in (17). First we note that the function $d(k) = \ln(|\lambda_k|)$ is by definition always negative. $d(k)$ is defined on a discrete lattice (integer k) and $d(k) = d(-k)$. Let us consider $k \geq 0$. Then $d(k)$ has a single maximum either for one value of $k = k_m$ or for two subsequent values $k = k_m$ and $k = (k_m + 1)$. For $k \geq k_m$ the function $d(k)$ is monotonically decreasing with increasing k. Then the linearization in (25) is violated for a given k_0 if there exists a sequence of $k_1, k_2, \ldots, k_{\alpha-1}$ such that

$$d(k_0) \leq [d(k_1) + d(k_2) + \cdots + d(k_{\alpha-1})] \tag{28}$$

holds together with the condition [see (17)]

$$k_0 = \pm k_1 \pm k_2 \pm \cdots \pm k_{\alpha-1} \quad . \tag{29}$$

The reason is that in this case a given nonlinear combination is decaying in space more weakly than the corresponding linear term.

Since Eqs. (28) and (29) can never be satisfied for $k_0 = k_m$ it follows that the linearization is always jus-

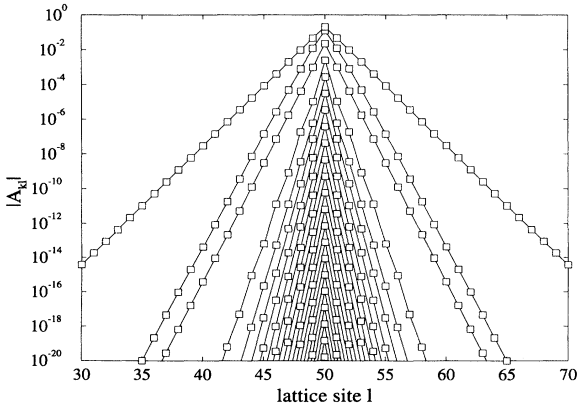

FIG. 3. Same as in Figs. 1 and 2 but for an XC NLE solution of model II.

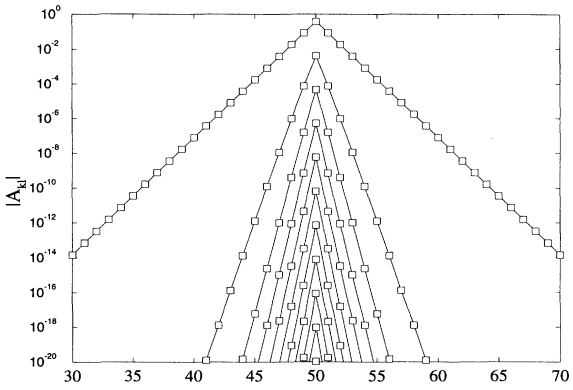

FIG. 4. Same as in Figs. 1, 2, and 3 but for an XC NLE solution of model III.

tified for k_m. Let us consider $k > k_m$. If the sequence of $(k_1, k_2, ..., k_{\alpha-1})$ yields a violation of the linearization, then all k numbers from this sequence have to be of lower value than k. Increasing k step by step starting from k_m we can then account for all possible nonlinear corrections of the result of linearization. Since $d(k) \sim -2\ln(k)$ for large values of k, it follows from a numerical analysis that for each value of α there will be a k_+ such that no nonlinear corrections appear for $k > k_+$. Also for a given function $d(k)$ there will be a α_+ such that no nonlinear corrections appear for any value of k.

Let us consider the numerical results for NLE's from the preceding section in the light of the above given considerations. The case shown in Fig. 1 was analyzed in [3]. Figure 5 in [3] shows very good agreement between the k-dependent exponents of the decay as found from the numerical solution (Fig. 1) and the result of the linearization. A careful check of the nonlinear corrections indeed shows that the linearization result holds without exception. The same result is valid for the XN NLE in Fig. 2.

The XC NLE solution shown in Fig. 3 cannot be described in its decay properties by the linearization result only. In Fig. 5 we show the exponents as calculated from Fig. 3 (squares) and the predicted exponents from the linearization procedure (filled circles). Clearly for $k = 2$ (and also less visibly for $k = 3$) the numbers differ. The exponents for the solution are

k	num. result	linearization
0	-1.3202	-1.3415
1	-0.6904	-0.6898
2	-1.3796	-1.6588
3	-2.0748	-2.1143
4	-2.3957	-2.3951
5	-2.6018	-2.6026
6	-2.7663	-2.7682
⋮	⋮	⋮

Nonlinear corrections can appear from terms with $\alpha = 3, 4$. For $\alpha = 3$ we can find the following corrections. For $k = 2$ the nonlinear contribution $A_{1l}A_{1l}$ yields an exponent $(-0.6904 - 0.6904) = -1.3796$, which is exactly what is found from the numerical result and is larger than the value of the linearization result -1.6588. The sign of A_{2l} should alternate according to the linearization result. If the nonlinear terms in (25) dominate, the sign of $A_{2l} \sim -A_{1l}^2$ should be negative — exactly as found from the numerical result (cf. the preceding section). For $k = 3$ the nonlinear contribution $A_{1l}A_{2l}$ (with the corrected exponent for A_{2l}) yields an exponent $(-0.6904 - 1.3796) = -2.0700$ which is again very close to the numerical result and larger than the linearization result -2.1143. The sign of A_{3l} should alternate according to the linearization result. If the nonlinear terms in (25) dominate the sign of $A_{3l} \sim -A_{1l}A_{2l}$ should be positive ($A_{1l} > 0$ is found from the numerical solution) — exactly as found from the numerical result (cf. the previous section). The only nonlinear contribution from the nonlinear term with $\alpha = 4$ appears for $k = 3$ (A_{1l}^3) and is equivalent to the $\alpha = 3$ contribution ($A_{1l}A_{2l} = A_{1l}A_{1l}^2$) with respect to the value of the exponent as well as with respect to the sign of the correction. For $k > 3$ no nonlinear corrections are found — consequently the linearization result coincides with the numerical findings both in the value of the exponent and in the sign of the Fourier components (alternating).

The XC NLE solution shown in Fig. 4 also has nonlinear corrections in the spatial decay. In Fig. 6 we show the exponents as calculated from Fig. 4 (squares) and the predicted exponents from the linearization procedure (filled circles). For $k = 3$ the results are different. The exponents for the solution are

k	num. result	linearization
1	-0.6722	-0.6709
3	-1.9910	-2.1464
5	-2.6103	-2.6133
7	-2.9114	-2.9117
9	-3.1324	-3.1325
⋮	⋮	⋮

Only nonlinear terms with $\alpha = 4$ are present. For $k = 3$ the nonlinear contribution $A_{1l}A_{1l}A_{1l}$ yields an exponent $(-0.6722 - 0.6722 - 0.6722) = -2.0166$ — very close

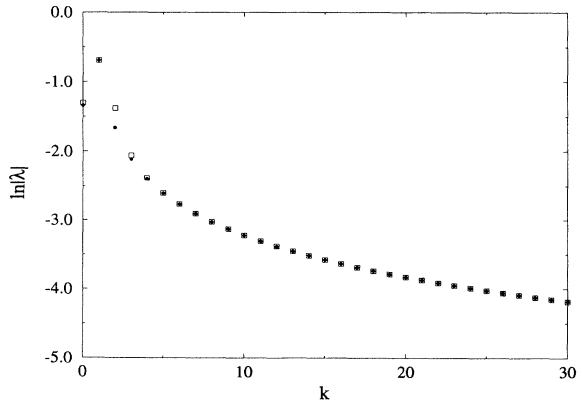

FIG. 5. Exponents of the spatial decay $\ln|\lambda|$ as a function of k for the NLE solution shown in Fig. 3. Open squares: numerical result, filled circles: linearization result.

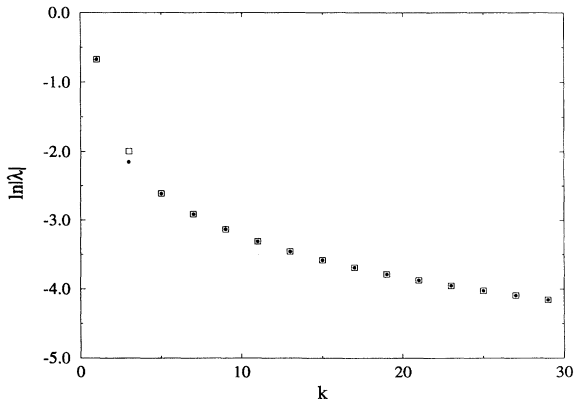

FIG. 6. Same as in Fig. 5 but for the NLE solution shown in Fig. 4.

to the numerical result and larger than the value of the linearization result -2.1464. Since the sign of A_{1l} alternates, so does the sign of $A_{3l} \sim A_{1l}^3$. For all other $k \neq 3$ the nonlinear terms give no corrections to the linearization result.

Nonlinear corrections can be expected if one of the multiples of the frequency $\tilde{k}\omega_1$ comes close to the phonon band — then the corresponding spatial decay exponent comes close to zero and can easily contribute to the decay properties of Fourier coefficients with, e.g., $k = (\alpha - 1)\tilde{k}$.

VI. THE DECAY IN k SPACE

So far we have considered the spatial decay of NLE solutions. However, as was already explained, in order to obtain numerical solutions we have to introduce a cutoff in k space. This cutoff will only be justified if the Fourier components decay in the k space. From the examples in Figs. 1–4 this decay is clearly visible. In this section we will obtain some analytical results for the decay in k space for a solution where no nonlinear corrections to the linearization result (of the spatial decay, see preceding section) appear.

As it appears from (27) the k dependence of the Fourier coefficients is given by

$$A_{kl} \sim s(k) e^{-\ln(|\lambda_k|)|l|} , \tag{30}$$

where the function $s(k)$ describes the k dependence of the Fourier coefficients at lattice site $l = 0$ (for convenience we assume that the NLE is created with center at $l = 0$; in case of reference to numerical results a shift in the lattice site numbers is implied). If we consider the XC NLE solution in Fig. 1, then we observe that $\ln[s(k)] \sim -k$. For large values of k

$$\lambda \approx -\frac{\omega_1^2 k^2}{\phi_2}$$

and consequently

$$|A_{kl}| \sim k^{-2|l|} s(k) . \tag{31}$$

In the case of Fig. 1 this implies that the decay of the Fourier components in k space is given by the product of an exponential decay and a power law decay, where the power law decay is lattice site dependent — the farther from the center of the NLE, the larger the exponent of the power law decay. In fact, according to (31) the exponent of the power law decay should increase by 2 as one switches from a lattice site to its nearest neighbor.

In Fig. 7 we plot the normalized Fourier components $|A_{kl}|/s(k)$ from Fig. 1 as a function of k in a log-log plot. Data with the same values of l are connected with lines. Clearly power laws are observed. In Fig. 8 the l dependence of the power law exponent is shown by plotting the differences between power law exponents on neighboring lattice sites — as predicted this difference appears to be approximately -2 (deviations for larger values of l appear because of the smallness of the unrenormalized Fourier coefficients).

From the results in this section we can conclude that the decay of the Fourier components in k space is faster as the distance from the NLE center increases.

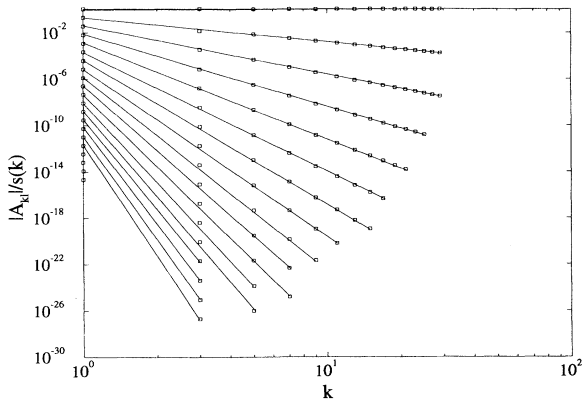

FIG. 7. k dependence of the Fourier coefficients of the NLE solution shown in Fig. 1. Here the Fourier coefficients are renormalized using the data for the central particle. The result is plotted in a log-log plot. Open squares: numerical data. Lines: best eye fit of a power law (straight line in the plot) for every lattice site l.

VII. A VARIATIONAL APPROACH

So far we have implemented a numerical method of obtaining NLE solutions and have used the numerical results in order to verify and improve several analytical findings. For completeness we show in this section that NLE solutions can be obtained out of a variational problem, i.e., we can define a function of the Fourier coefficients such that a NLE solution will correspond to an extremum of this function. This result can be useful both in considering an independent method of finding numerical NLE solutions as well as in performing existence proofs for NLE's in lattices with dimensions higher than 1 and in considering the analogous properties of quantum lattices.

Let us consider the action S of a given classical lattice:

$$S = \int_0^t d\tau L , \tag{32}$$

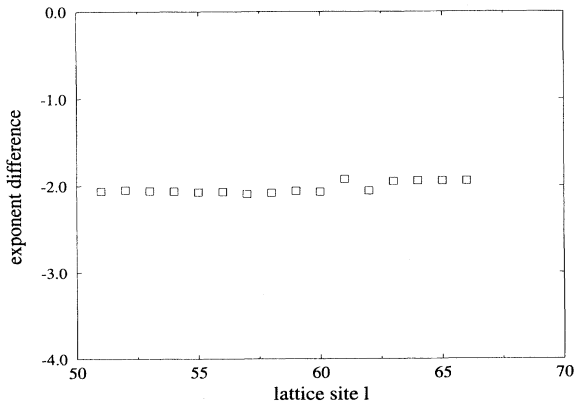

FIG. 8. The difference of the power law exponents for the k dependence of the Fourier coefficients for neighboring lattice sites as obtained from Fig. 7.

where the Lagrange function L is given by

$$L = \sum_l \dot{X}_l^2 - H \ , \tag{33}$$

and the Hamilton function H is given in (1). We search for a periodic solution (closed trajectory) with period $t = 2\pi/\omega_1$. Inserting (6) into (32) and integrating over the period we find for the action S_p of a periodic solution

$$\begin{aligned} S_p \frac{\omega_1}{2\pi} = & \sum_l \sum_k \frac{1}{2} k^2 \omega_1^2 A_{kl} A_{-k,l} \\ & - \sum_l \sum_{\alpha=2}^{\infty} v_\alpha \frac{1}{\alpha!} \sum_{k_1,k_2,\cdots,k_\alpha} A_{k_1 l} A_{k_2 l} \ldots A_{k_\alpha l} \\ & \times \delta_{0,(k_1+k_2+\cdots+k_\alpha)} - \cdots \ . \end{aligned} \tag{34}$$

Here the final $\cdots$ in (34) implies the evaluation of the interaction terms (4), which look similar to the second term of Eq. (34) except that the lattice site labels in one product can come from two neighboring lattice sites.

Let us consider the derivative of S_p with respect to a given A_{kl}:

$$\begin{aligned} \frac{\omega_1}{2\pi} \frac{\partial S_p}{\partial A_{kl}} = & \ k_2 \omega_1^2 A_{-k,l} - \sum_{\alpha=2}^{\infty} v_\alpha \frac{1}{(\alpha-1)!} \\ & \times \sum_{k_1,k_2,\cdots,k_{\alpha-1}} A_{k_1 l} A_{k_2 l} \ldots A_{k_{\alpha-1} l} \\ & \times \delta_{0,(k+k_1+k_2+\cdots+k_{\alpha-1})} - \cdots \ . \end{aligned} \tag{35}$$

Now we observe that if a periodic solution on the lattice is found, i.e., if Eq. (10) holds, then for these solutions the right hand side of (35) vanishes [if one replaces k by $-k$ in (10)]. Consequently the function S_p from (34) has to have an extremum with respect to variations of the Fourier coefficients A_{kl} for a periodic solution. Also the inverse is true: if S_p has an extremum with respect to variations of the Fourier coefficients

$$\frac{\partial S_p}{\partial A_{kl}} = 0 \tag{36}$$

for all (kl) then the set of Fourier coefficients which corresponds to this extremum is a periodic solution of the equations of motion.

VIII. DISCUSSION

We have shown the construction of a map for the Fourier coefficients of a periodic solution on a lattice. This map is specifically designed to obtain spatially localized time-periodic solutions. The usefulness of this method is first that very little (in fact nothing specific) has to be known about the solution one searches for, i.e., the initial condition (starting distribution of the Fourier coefficients) has to reflect only the localized character of the solution one looks for. This circumstance makes our approach much easier than, e.g., the approach used in [10]. There, also, a map was designed to obtain localized time-periodic solutions. However, the initial condition had to be chosen to be very close to the final result. In other words, one had to obtain information about the final solution before even starting the map.

Second, with our method we derive final solutions with high numerical precision. This precision allows for the numerical analysis of several problems, e.g., the dynamical stability of the derived solutions, the study of scattering events of plane waves by the localized solutions, and others. Let us explain this using the scattering problem. In [11] the scattering (reflection) of phonon waves by a single localized solution was studied for a one-dimensional lattice. The maximum amplitude for the localized solution was of the order of 1, and the errors of the amplitudes for the same solution were of the order of 10^{-3} leading to uncertainties in the energy distribution of order 10^{-6}. The in-falling phonon wave had to have an energy density of the order of 10^{-4} in order to ensure nearly linear dispersion. The transmission of phonons was increasingly suppressed with increasing wave number. Since the squared transmission coefficient was observable only for values down to 10^{-2}–10^{-3} the maximum wave number under study was around $0.4 q_{ZB}$ (here q_{ZB} means the zone boundary wave number). With the accuracy of the final solutions as derived in this work (10^{-15} in amplitudes, 10^{-30} in the energy density) one should be able to trace the squared transmission coefficient down to values of 10^{-20}–10^{-26} which implies that nearly the whole Brillouin zone can be studied.

Of course the presented method can be used in lattices with dimension larger than 1, too. The analysis of the solutions, however, will be much more tedious; thus we have demonstrated the method using one-dimensional systems. The formulation of the variational approach in the previous section can also be useful in lattice dimensions higher than 1.

We have used the results obtained with this method to test predictions of analytical considerations of the spatial decay of a localized vibration. As a result we found that nonlinear corrections of a linearization method used to account for the exponential decay appear if a multiple of the fundamental frequency of the localized solution comes close to the phonon band. We have further shown how these nonlinear corrections can be obtained analytically and found very good agreement with the numerical results. This part of the work was also carried out for one-dimensional systems. It is possible to analyze higher dimensional lattices with this method too. For that one has to consider lattice Green's functions (see, e.g., [12, 13]). These functions will appear if one deals with the equations for the Fourier components of a localized vibration on a given lattice [the equations are essentially as in (10)]. Far away from the center of the NLE one can again linearize these equations. The lattice Green's functions can be used then in order to obtain analytical solutions. The k-dependent spatial decay will be obtained, and nonlinear corrections can be considered in full equivalence to the cases analyzed in the present work.

Let us finally stress that the method and results obtained in this work can be used to perform a dynamical

stability analysis of the NLE solutions as indicated in [8]. The corresponding eigenvalue problem can be formulated in the space of Fourier coefficients. As an input of this stability analysis one needs precise data on the Fourier coefficients of the periodic NLE solution, which are provided by the presented method.

ACKNOWLEDGMENTS

It is a pleasure to thank C. R. Willis, E. Olbrich, and K. Kladko for interesting and stimulating discussions, and C. R. Willis and P. Fulde for a critical reading of the manuscript.

[1] A. J. Sievers and S. Takeno, Phys. Rev. Lett. **61**, 970 (1988).
[2] S. Takeno, J. Phys. Soc. Jpn. **61**, 2821 (1992).
[3] S. Flach, Phys. Rev. E **50**, 3134 (1994).
[4] S. Flach, Phys. Rev. E **51**, 1503 (1995).
[5] R. S. MacKay and S. Aubry, Nonlinearity **7**, 1623 (1994).
[6] S. Flach, C. R. Willis, and E. Olbrich, Phys. Rev. E **49**, 836 (1994).
[7] S. Flach and C. R. Willis, Phys. Rev. Lett. **72**, 1777 (1994).
[8] S. Flach, K. Kladko, and C. R. Willis, Phys. Rev. E **50**, 2293 (1994).
[9] J. H. Wilkinson, *The Algebraic Eigenvalue Problem* (Oxford University Press, New York, 1992).
[10] D. K. Campbell and M. Peyrard, in *CHAOS — Soviet American Perspectives on Nonlinear Science*, edited by D. K. Campbell (American Institute of Physics, New York, 1990).
[11] S. Flach and C. R. Willis, in *Nonlinear Excitations in Biomolecules*, edited by M. Peyrard (Springer-Verlag, Berlin, 1995).
[12] S. Takeno and K. Hori, J. Phys. Soc. Jpn. **60**, 947 (1991).
[13] T. Dauxois, M. Peyrard, and C. R. Willis, Physica D **57**, 267 (1992).